Kurdistan Journal of Applied Research (KJAR)
Print-ISSN: 2411-7684 | Electronic-ISSN: 2411-7706

Original Article

Check for updates

Expression and Purification of the Full Length and N-Terminal Truncated Variants of Insect CYP6Z2 in the Cytosol of Escherichia Coli for Potential 3D Experimental Studies

Michael Olugbenga Kusimo [a,b,c*], **Taib Ahmed Hama Soor** [c,d], **Ahmed Adebowale Adedeji** [e]

[a] Society Empowerment for Transformation Initiative (SETI), Rumukurushi, Port-Harcourt, Nigeria.
[b] Foresight Institute of Research and Translation,93 KK 31, Gikondo, Rwanda.
[c] Department of Molecular Biology and Biotechnology, University of Sheffield Western Bank Sheffield, UK.
[d] Medical Laboratory Department, College of Health and Medical Technology, Sulaimani Polytechnic University, Sulaymaniyah, Iraq.
[e] Department of Pharmacology and Toxicology, School of Medicine and Pharmacy, College of Medicine and Health Sciences, University of Rwanda, Rwanda.

Submitted: 19 August 2023
Revised: 28 September 2023
Accepted: 30 December 2023

* **Corresponding Author**: gkusimo@gmail.com

Keywords: Cytochrome P450, insecticide resistance, protein folding, structural stability, 3D structure

How to cite this paper: M. O. Kusimo, T. A. Hma Soor, A. A. Adedeji"Expression and Purification of the Full Length and N-Terminal Truncated Variants of Insect CYP6Z2 in the Cytosol of Escherichia Coli for Potential 3D Experimental Studies", KJAR, vol. 8, no. 2, pp. 61-70, Dec. 2023, doi: 10.24017/science.2023.2.6

Abstract: Cytochrome P450 enzymes (P450s) offer innate resistance defence for malaria vectors against the insecticides permitted by WHO to be used in vector control tools. P450s can detoxify broad substrates and simultaneously metabolise them, thus the availability of experimental three-dimensional structures of these key insecticide detoxifiers is vital to improving our knowledge of their enzyme activities. Despite the importance of this family of proteins in insecticide resistance, there are no available experimental three-dimensional structures of insect P450 yet. For this investigation, a carboxy-terminal Histidine-tagged recombinant CYP6Z2 was heterologously expressed in *E. coli* to generate a soluble holoprotein suitable for an experimental three-dimensional structure. The expressed enzyme was purified from the cytosol of *E. coli* via the combination of various purification techniques and cholic acid sodium salt. Two truncated N-terminal signal peptides: short deletion of 11 amino acids and long deletion of 23 amino acids of the hydrophobic domain, were created to prevent aggregation, improve solubility, and facilitate crystallisation. The CYP6Z2 (full length) produced a holoprotein with a P450 protein concentration of 0.60 nmol/mL, whereas the two truncated CYP6Z2 isoforms produced only the inactive species with no peak at 450 nm. We conclude that the hydrophobic signal peptide region of the insect Cytochrome P450s seems sensitive and indispensable to ensuring 3-D folding and stability.

1. Introduction

Pyrethroid and other insecticide resistance bestowed on malaria vectors by P450s is a major setback to improving the fight against malaria disease using vector control tools [1]. The WHO reports

revealed that more than three billion individuals may be at risk of being victims of mosquito bites resulting in malaria disease and death [2, 4]. This possible loss of lives drives the attempts to unravel the 3D structure of these P450s. However, no experimental 3D structure of these important insect P450s has been determined. Insights into the 3D topology of these insect P450s are only possible via homology modelling [5-7] using experimentally determined 3D structures, such as human CYP3A4, which shares less than 24% amino acid similarity [8, 9]. While the sequence of the amino acids constituting the catalytic domain configuration of known P450s is preserved, the side chains' spatial orientations in the few P450s with determined 3D structures vary [10]. These dissimilarities underscore the significance of obtaining an experimental 3D topology of a prototype enzyme from each P450 family. This will facilitate a better understanding of how the structure of this insect P450 influences its ability to detoxify insecticides [11].

The 3D structural studies require high throughput of heterologous protein expression [12-14]. A bacterial protein expression system using *E. coli* is usually the expression system of choice to produce a good quantity of starting material for structural study. Eukaryotes P450s are localized in the membrane, thus the heterologous expression of these enzymes in *E. coli*, which lack the proper compartmentation of organelles, naturally produces low protein yield. Conversely, the eukaryotes possess an internal membrane arrangement suitable to house the huge microsomal enzymes [15]. More significant is the consequence of the hydrophobic signal peptide of the N-terminal domain of these eukaryotic enzymes on their solubility in the cytosol of *E. coli* [16].

The foremost P450 enzyme produced in quantity adequate for the 3D experimental study was Cytochrome P450cam from *Pseudomonas putida*: a prokaryote [17]. The absence of N-terminal hydrophobic peptide in prokaryotes is believed to be an important feature that improves their solubility in the cytosol, therefore, [18] the crystal structure of P450-BM3 was determined six years after that of P450-CAM. Consequently, additional crystal structures of prokaryotic P450s have been resolved, providing useful templates for the 3D-homology modelling of unresolved eukaryotic P450s [11]. The foremost experimental 3D structure of mammalian P450 to be resolved was that of the rabbit CYP2C5 [17]. The N-terminal signal domain was removed and a chimeric protein containing amino acid residues from CYP2C3 was generated. The amino acid residues replaced were recognized to enhance the oligomerization of the translated chimeric version of CYP2C5 to a monomer, using high-salt buffers without the addition of detergent [19]. Conducting only the mutagenesis of the N-terminal transmembrane domain for CYP2C3 and CYP2C5 translated as dimers and tetramers, respectively, when their expressions were processed using a buffer with high salt concentration [20]. Consequently, the molecular manipulation of the N-terminal truncations and alterations has made feasible the possibility for additional eukaryotic P450 crystal structures of 2B, 2C, and 3A subfamilies [11, 21-24]. Nevertheless, the crystal structure of CYP3A4 in humans was effectively resolved by just truncating its N-terminal signal peptide, without any other alterations [24].

This study aimed to advance the methodology to express and purify the intact *Anopheles gambiae* CYP6Z2 with its N-terminal signal peptide as a soluble protein in *E. coli* cells. Additionally, it sought to determine the effect of deleting the N-terminal signal peptide, as done with human CYP3A4, on the structural conformation and expression of the resulting mutated isomers. Two N-terminal truncations: 11 and 23 amino acids were genetically engineered and cloned into the pB13 plasmid. The folding pattern of the holoprotein of the two N-terminal truncated P450s was monitored and compared with the full protein.

2. Materials and Methods

2.1 Reagents

New England Biolabs (NEB) supplied the Phusion High Fidelity Polymerase used in this study. Eurofins genomics synthesised the oligonucleotides and other enzymes used for the DNA engineering were purchased from Thermo Fisher Scientific. Aminolevulinic acid (ALA), Isopropyl-ß-D-thio-galactopyranoside (IPTG), 3-[(3-cholamidopropyl) - dimethylammonio]-1-propanesulfonate (CHAPS) and 5-aminolevulinic acid (ALA) were purchased from Melford (UK). Ni2+-NTA was purchased from

Invitrogen. The ECL kit reagent was supplied by GE Healthcare, and the Bradford reagent was purchased from BioRad.

2.2 Construction and Cloning of the N-TerminalTruncated Versions Of 5x His-Tagged CYP6Z2

pB13 plasmid construct expressing His-tagged CYP6Z2 was cloned without the ompA peptide as performed by McLaughlin *et al*., 2008 [8]. This recombinant CYP6Z2 with 5 histidine codons at the 3' end was utilised as a template to create the two N-terminal truncated versions employing Phusion High Fidelity Polymerase. The primers were designed to retain the NdeI restriction site, start codon, and nucleotide sequences starting from the 12th and 24th amino acid codons of the CYP6Z2 template (Table 1) for the short and long truncations, respectively. The product from the PCR was cut from a 1% agarose gel and purified using a gel extraction kit supplied by Qiagen. The purified amplicon and pB13-CYP6Z2 were then digested using Nde1 and EcoR1 to generate matching sticky ends on the DNA sequences of the truncated PCR amplicons and the pB13 plasmid. The overnight digestion of the two was processed at 37 °C and the reaction mixtures were then loaded on 1% agarose gel. The bands were cut out of the agarose gel, purified as stated above and then ligated using the T4 ligase. The ligated re-engineered plasmid was used to transform DH5α competent cells and incubated at 37 °C overnight. The recombinant plasmids were recovered and sent for sequencing.

Table 1: The primers used with CYP6Z2 sequence to create the truncated variants of 5x His-tagged CYP6Z2.

	Forward primer	**Reverse primer**	**Number of residues deleted**
5xHis-tagged CYP6Z2(Δ3-25)	5'CAT**ATGGCT**GGACT TCCTCATCTAAAGCC AGA 3'	5'CCGGGAATTCTCAATGG TGATGGTGATG 3'	23
5xHis-tagged CYP6Z2Δ3-13	5'CAT**ATGGCT**TTTCT CGTGCTCCGCTACAT CTA-3'	5'CCGGGAATTCTCAATGG TGATGGTGATG 3'	11

2.3 Expression of the Intact 5x His-Tagged CYP6Z2 and the Two Truncated Variants

An adapted method of the procedures used for the production and purification process of the CYP2B subfamily [11] was exploited to study the expression of the full-length CYP6Z2 and the truncated variants. *E. coli* JM109 K cells were transformed with the verified plasmid and grown on ampicillin plates. A colony from the transformation process was added to a 20 ml luria broth (LB) augmented with ampicillin to a final concentration of 100 μg/ml. The LB in a 500 mL flask was incubated at 37 °C with shaking at 200 RPM overnight. After the incubation, 15 ml was added to a terrific broth of 250 ml in a 2 L flask augmented with 100 μg/ml ampicillin. The growth of the cells was monitored at 600 nm to reach an optical density of 1–1.5 at 37 °C. The protein translation was initiated with 1 mM IPTG and ALA at 80 mg/litre. Additionally, 5 mM Imidazole was included in the solution at the time of inducting protein expression to sustain the formation of the holoprotein. The incubating culture was allowed to grow for 24 hrs at a temperature of 30 °C while shaking at 120 RPM. The growing cells in the culture were collected by centrifugation at 5000 RPM for 15 minutes at 4 °C using a JA-14 fixed angle rotor of a Beckman JA-21 centrifuge. The production of the protein was monitored at different growth conditions and the production of properly folded P450 enzyme was compared.

2.4 Affinity Chromatography of the Intact 5X His-Tagged CYP6Z2

Purification of the protein was carried out at a temperature of 4 °C. The centrifuged cell pellets from the culture were resuspended in 500 mM potassium phosphate, 10 mM β-mercaptoethanol (β-ME), 10 % glycerol, and 0.4 % sodium cholate at pH 7.4 and then homogenised. The well-homogenised cell suspension was sonicated for 30 seconds and then cooled on ice for 45 seconds. This process was repeated three times. The sonicated solution was centrifuged for 35 mins at 113,000 g (31,000 RPM)

utilising a fixed-angle Ti 50.2 rotor in a Beckman Ultracentrifuge machine. The supernatant was loaded onto Ni2+-NTA resins previously equilibrated using 500 mM potassium phosphate buffer, 10 mM β-ME, 10 % glycerol, and 0.4 % of the detergent: sodium cholate at pH 7.4. Then a β-ME buffer solution (buffer solution A: 10 mM β-ME, 500 mM potassium phosphate, and 10 % glycerol) was utilised for the washing steps. The sample loaded on the resins was cleaned using the following solutions: 1st buffer- 500 mM buffer solution A at pH 7.4 fortified with 0.1 % sodium cholate detergent, second buffer- 10 mM buffer solution A at pH 7.4 plus 20 mM imidazole, and third buffer- 10 mM solution A at pH 7.4 plus 40 mM imidazole reagent. The purified protein was eluted from the column using 10 mM buffer solution A at pH 7.4 with 500 mM imidazole plus 0.5 M NaCl included in the buffer used to elute the protein. The eluted fractions were collected and analysed on SDS-PAGE. These fractions collected were then examined using Western Blotting. The fractions were pooled into a dialysis bag and dialysed in a litre of 10 mM potassium phosphate at pH 7.4 and 100 mM NaCl.

2.5 SDS-PAGE Analysis

A resolving gel of 10% was utilised to analyse the purified enzyme. The gel was run in 1 x SDS-Page running buffer (3.03 g/L tris base, 14.4 g/L glycine, and 1 g/L SDS pH 8.3) for the first 10 mins at 80 V to allow the sample to stack properly on the resolving gel and then the voltage was increased to 100 V for 60 mins. A pre-stained protein ladder ranging from 15 -150 kD was added to the gel and run alongside the purified fractions. The resolved SDS gels were processed for both staining with Coomassie and western blotting.

2.6 Ion Exchange Chromatography

The computed isoelectric point (pI) (https://web.expasy.org/compute_pi) of the intact CYP6Z2 (5H) was 8.04, at pH 7.4, suggesting that the enzyme would carry a net positive charge under these conditions. Both cationic (SP Sepharose) and anionic (Q Sepharose) ion exchange chromatography were utilised to improve the purity of the intact 5x His-tagged CYP6Z2. The separating funnel was loaded with 500 uL of Q-sepharose and then equilibrated thoroughly with phosphate buffer (pH 7.4) before loading the sample. The expressed protein unexpectedly stayed on the Q-sepharose and did not flow through. The bound sample was then eluted with phosphate buffer (pH 7.4) supplemented with 500 nM NaCl. Conversely, the expressed protein did not bind to SP Sepharose and thus ran through the column while other impurities stayed on the column; therefore, the protein was collected without eluting it with NaCl.

2.7 Immunoblotting

A nitrocellulose membrane of 0.2 μm pore size was cut into the same measurement as the resolving gel and they were placed together in the cassette of the immunoblotting tank. A Tween-PBS (TPBS) buffer was added to the tank and processed for 90 minutes at a current of 200 mA. The nitrocellulose paper was removed and blocked using 1% BSA added to the T-PBS buffer at room temperature for a period of 1 hr. The antibody: Hisprobe-HRP, added to 1% BSA in the TPBS buffer, was replaced with the previous buffer and then incubated for another 1 hr. T-PBS was then used to rinse the membrane, followed by further rinsing with PBS only to clear the detergent. The antibody probe was developed using an ECL reagent kit according to the manufacturer's instructions. The blots on the membrane were captured in the darkroom on X-ray film.

2.8 Bradford Assay

The expressed and purified enzyme was quantified using a Bradford reagent and measured at 595 nm [25]. Known concentrations of BSA were utilised to create a protein standard curve. The quantity of the expressed protein was then deduced through interpolation on the standard curve. The purified protein was diluted 100-fold before quantifying it to be read on the standard curve.

2.9 Evaluation of the P450 content of the 5x His-Tagged CYP6Z2 Produced

The synthesis of the P450 expressed was tracked in JM109 cells by taking 1 ml of the broth culture and centrifuging it at 4 °C and a speed of 16,000 RPM. The supernatant was discarded and the pellet dissolved in 1 ml of previously prepared P450 spectrum buffer (20% glycerol in PBS). This was vortexed to mix and then 500 μL each was added into two dark quartz cuvettes labelled 'B' for blank and 'E' for experiment. The recombinant P450 that folded properly in the cells was tracked using Fe2+-CO vs. Fe2+ difference spectra as described [26]. We used the same steps to estimate the expressed P450 content.

3. Results

3.1 Molecular Engineering of the Intact and Truncated 5x His-Tagged CYP6Z2 Variants

The full-length CYP6Z2 amplified from previously described pB13ompACYP6Z2 construct [8], sub-cloned without the ompA but with 5x His-tagged to the C-terminus, yielded a distinct amplicon. Nde1 cut the 5' and EcoRI cut the 3' end. The digested products have a length of 1.5 kbp for the insert and 5 kbp for the pB13 plasmid when analysed on 1% agarose gel. A similar amplicon length was obtained after deleting the hydrophobic peptide region of the 5' end of the CYP6Z2.

3.2 Expression of the 5x His-Tagged Intact CYP6Z2 Protein and the N-Terminal Deleted Variants

The holoenzyme of the P450 expressed was tracked using a variety of growth settings. The truncated isoforms yielded only inactive species with no peak at 450 nm in all of the conditions used. The translation of the intact CYP6Z2 at a temperature of 25 °C with shaking at the speed of 150 RPM generated 33.18 nmol/l holoprotein after incubation for 24 hrs. The yield improved by 3.9-fold when expressed at 48 hrs, however, the P450 expressed unfolded and diminished at 72 hrs. Cells growing at 30 °C and shaking speed of 200 RPM produced 0.15 nmol/mL P450 after the incubation for 24 hrs but this increasingly reduced by 1.2-fold at 48 hrs and to 1.5-fold after 72 hrs. The 3rd growth settings of 30 °C and shaking speed of 120 RPM produced 0.12 nmol/mL P450 after 24 hrs incubation and gradually increased from 2.60-fold when grown for 48 hrs to 5.30-fold after 72 hrs of incubation (Figure 1).

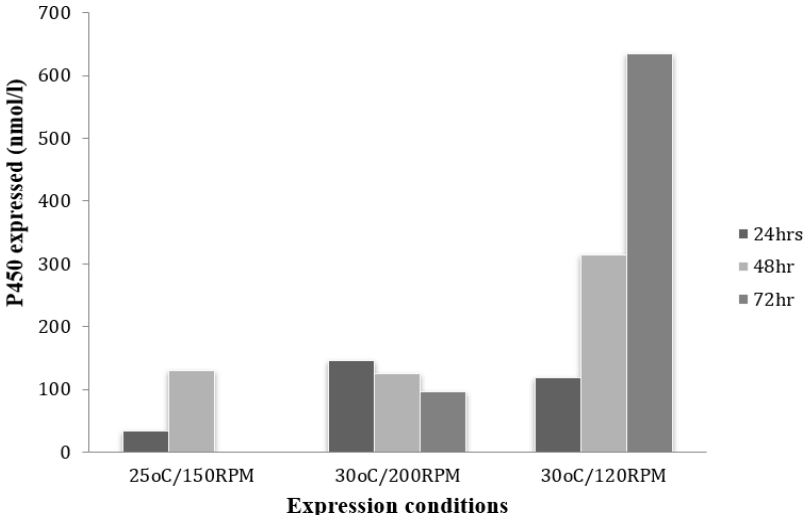

Figure 1: The quantity of the P450 expressed at various growth conditions. The P450 produced at 30 OC and shaking at slower RPM yielded the maximum protein concentration.

The intact CYP6Z2 synthesized a P450 holoprotein; nonetheless, the expression also presented a peak at 420 nm, demonstrating that a portion of the protein was unfolding. However, the deleted N-terminal variants yielded no properly folded P450 at 450 nm peak. The signal at 420 nm also indicated that the variants had low translation compared to the intact proteins (Figure 2). The intact CYP6Z2 yielded a P450 protein concentration of 0.6 nmol/mL.

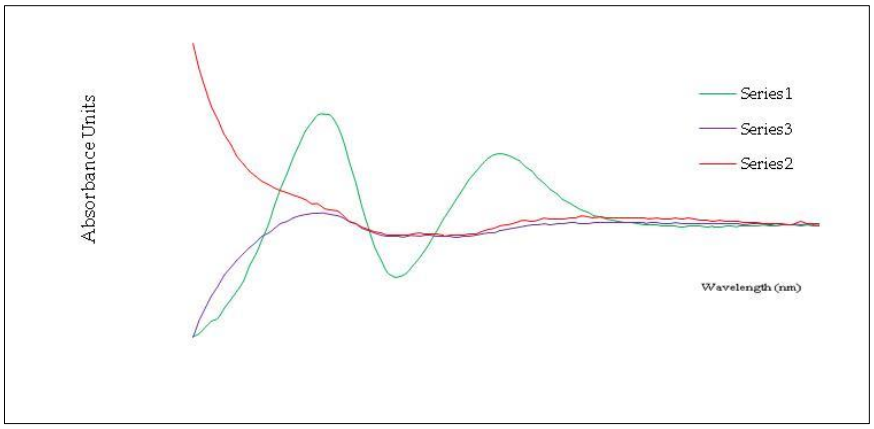

Figure 2: The difference spectra (Fe2+-CO vs Fe 2+) of the intact CYP6Z2 with the two truncated variants.

The plot showed the full-length CYP6Z2 with a peak at 450 nm confirming properly folded P450. The short truncated NH2-terminal sequence (Δ3-13) and the full deletion of the hydrophobic signal peptide (Δ3-25) did not fold properly.

3.3 Western Blotting of the Translated Full-Length 5x His-Tagged CYP6Z2

The comparatively huge hydrophobic nature of these detoxification enzymes, particularly at the N-terminal signal peptide, was a serious concern when the experimental design was being considered for the expression and purification of CYP6Z2 as an insect P450 prototype in the cytosol of *E. coli* for possible experimental 3D crystal structure trial. The N-terminal of P450s being expressed in bacterial cells was revealed to associate with the membrane, making the P450s insoluble in the cytosolic extracts [11]. Consequently, several procedures were examined to circumvent these complications to produce soluble P450. The quantity expressed was low when iron was added into the growing culture instead of ALA, the haem precursor. The procedure adopted by Modi *et al.*, 1996, utilising 20 mM Tris-buffer, 2 mM non-ionic detergent (CHAPS), and the haem precursor, ALA, to purify CYP2D6 [27], enhanced the protein yield, however, the translated protein unsuccessfully stayed on the Ni-NTA purification column as anticipated. B-mercaptoethanol (β-ME) was then added to the sample at this point before loading on the Ni-NTA affinity column. This breaks any disulfide bond holding the structure and exposes the histidine-tagged to the C-terminal for binding to the resin. The occurrence of contaminants after rigorous washing when implementing the Ni- NTA column purification phase (Figure 3B) shows the purified protein may have been degraded or the purified protein on the column may have pulled other lipoproteins with it, thus keeping them on the column.

The computational analysis of the isoelectric point of the translated protein of 5x His-tagged CYP6Z2 (gene length of 1.5 kbp as shown in figure 3A) indicated it has a net positive charge (pH 7.4). Nevertheless, when the experiment was performed by loading the sample on Q-Sepharose, an ionic exchanger, the protein stayed on the resin, demonstrating the sample has a net negative charge. We expected the protein to run through the column because the ionic exchange resins are positively charged and are supposed to attract the negatively charged impurities to remain on the resins in the column. This unexpected behaviour of the net charges of the sample as computed and what we observed when executing the separation on the column most likely is because of the presence of the P450 cofactor, the haem incorporated during the protein expression. Consequently, the sample went through SP Sepharose, cat-ionic exchange resins, as shown in figure 3C (SDS-PAGE) and figure 3D (nitrocellulose membrane), without staying on the column to produce a protein yield of almost 90% purity.

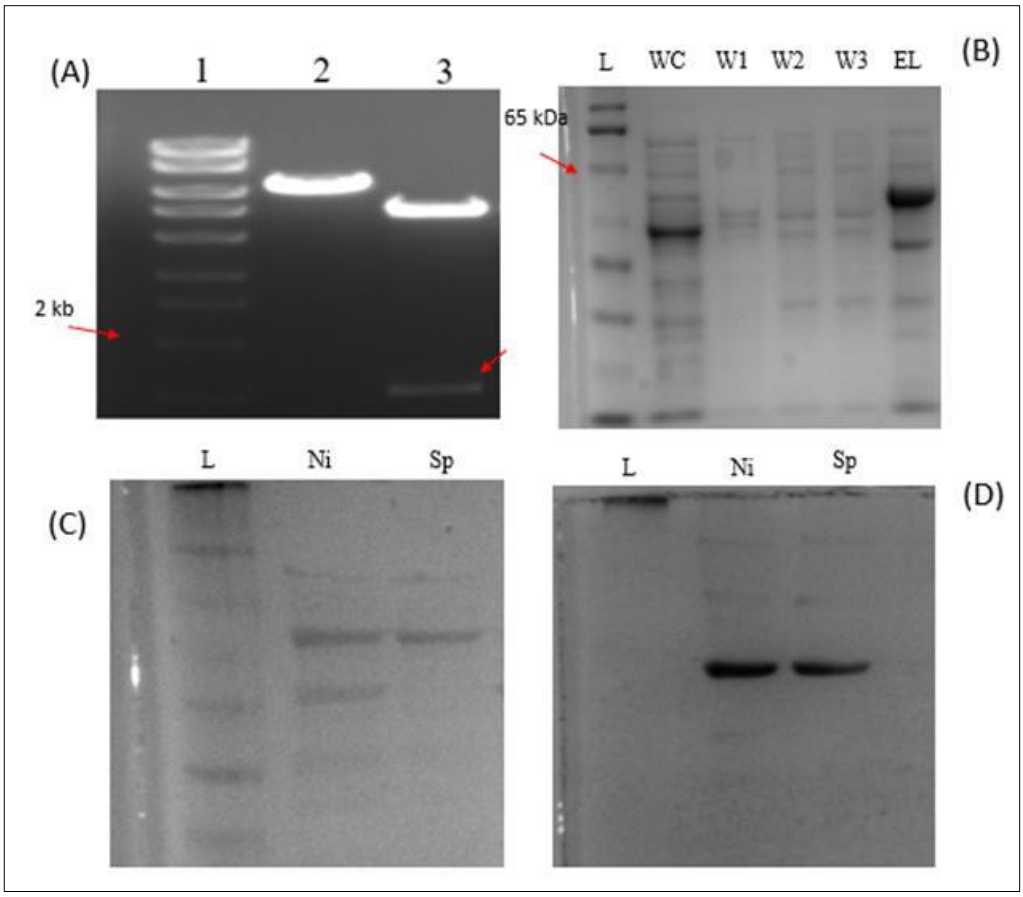

Figure 3: The cloning and expressed CYP6Z2 gene. (A) The image of the sample digested with endonucleases and DNA ladder-Hyperladder 1kb (Bioline) DNA markers on 1 % agarose gel. In lane 1 is the DNA ladder, lane 2 is a digested product using EcoR1, and lane 3 is the product of the double digestion using EcoR1 and Nde1 depicting the CYP6Z2 separated from the pB13 vector. The separated DNA sequence is 1.5 kbp and the plasmid sequence is 5 kbp. (B) The SDS-PAGE of the translated enzyme developed using Coomassie staining depicting the purification stages: pre-stained protein marker (L) -ladder-, (WC) whole cell lysate, (W1) first washing stage using 0.1% sodium cholate, (W2) second washing stage using 20 mM imidazole, (W3) third washing stage using 40 mM imidazole, and (EL) the elution stage using 500 mM imidazole. CYP6Z2 is approximately 56 kDa. (C) SDS-PAGE stained with Coomassie of the CYP6Z2 purification using affinity chromatography and additional purified using SP Sepharose resins: (L) is the protein ladder, (Ni) Ni-NTA affinity column and (SP) SP sepharose column. As seen on the SDS-PAGE the protein purity improved when further purification was done with the ion exchange chromatography. (D) Replica of the SDS PAGE to western blot on nitrocellulose membrane of 0.2 μm pore size. The experimental protocols generated a pure protein sample of 1.571 mg/ml. This was quantified using Bradford assay derived from the standard curve. The final P450 protein concentration computed from the difference spectra (Fe2+-CO vs Fe 2+) of the intact CYP6Z2 purified is 0.40 nmol P450/mg protein.

4. Discussion

This study is the first, to the best of our knowledge, to make available data attempting to produce the 3D structure of insect P450 and to establish the important role that the N-terminal signal peptide of insect P450s may be exhibiting in the proper folding of this enzyme. The 3D model of the insect CYP6Z2 illustrated (Figure4) reveals the topology with the extended hydrophobic N-terminal portion associating with the predicted 3D structure. Expressed microsomal P450s of eukaryotes are directed to the endoplasmic reticulum membrane via the signal peptide [28]. The hydrophobic domain also provides support by positioning the catalytic domain toward the cytoplasmic side [29]. The hydrophobic signal peptide poses an obstacle to the expression and solubilisation of the enzyme in the non-hydrophobic nature of the cytosolic environment of the prokaryote. The P450 enzymes will therefore form large protein aggregates after translation without a detergent [11]. While most P450 enzymes emerge as reduced aggregates when the hydrophobic signal peptide regions are truncated, they still emerge as oligomers after being purified. Monomers of such truncations could only be accomplished when detergents are used in the purification steps [11]. Although truncation of this trans-membrane region seems to be important for its solvability, it also seems significant for the 3D topology

of the insect P450s as seen in this study. According to Hsu *et al*.,1993 [30], the N-terminal of CYPC21 may be supporting the 3D structural prerequisite and stability of the protein [30]. This seems to be similar to the truncated CYP6Z2. Because the shorter length, keeping the peptide of the trans-membrane region that is close to the predicted 3D structure, also did not promote the expression of the enzyme.

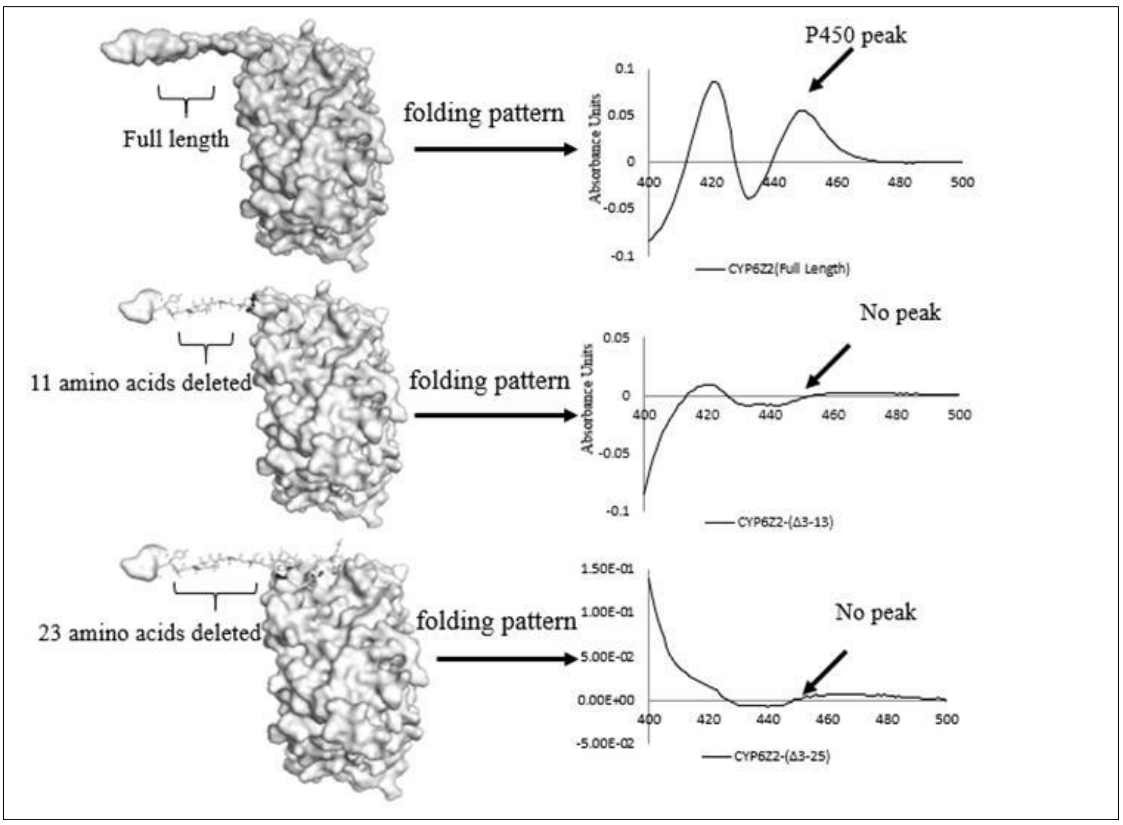

Figure 4: The CYP6Z2 homology models and the N-terminal truncated variants showing the folding pattern when expressed in *E. coli*. The partial and total deletion of the hydrophobic signal peptide produced improperly folded P450, suggesting this region interacting with the main domain may be essential for P450 catalytic structure

Nonetheless, the human CYP3A4 used for the experimental 3D study was possible with the deletion of the first 21 amino acid residues of the hydrophobic region which was expressed successfully in *E. coli* without additional mutation or modification to produce the crystal structure [24]. This structural study disclosed that CYP3A4 possesses an exceptional hydrophobic region, the 7 "phe-cluster" [23] and because hydrophobicity is one of the significant determinants of the folding of protein [31], CYP3A4 may not rely on its N-terminal hydrophobic domain for proper folding. In another experiment, numerous positively charged amino acid residues were added after truncating the N-terminal hydrophobic domain to increase translation and solubility as demonstrated in the expression of human CYP2B1 [11]. However, the outcome of this approach in promoting 3D structure was not revealed and a comparable alteration applied to CYP2B6 [32] did not increase the translation levels of this altered version more than the intact CYP2B6 in the cytosol of the prokaryotic cells [33]. The inclusion of these positively charged residues after deleting the signal peptide was proposed to increase the solubility of the enzymes by changing the subcellular position of the P450s to the cytosol [11, 34]. However, this method only reduced the P450 enzyme'sassociation with the *E. coli* membrane after truncation of the signal peptide and not necessarily for the proper 3D folding of the P450 being expressed.

Comparison of the sequences of the residues of the signal peptide of the insect CYP6Z2 with human CYP2C2 and CYP2B sub-family (Table 2) revealed a spacer sequence in between the signal domain and the rest of the 3D structure [29]. The spacer region is a glycine-rich part of the signal peptide among residues 22-28 with a proline-rich region between residues 30 to 37 which comprises a preserved

PPGP sequence [29]. Proline and glycine, together, are considered as α-helix breakers seen around bends aiding the 3D structural scaffolding of proteins [35]. The PPGP is preserved in CYP2B [11] and could be supporting the 3D topology of the modified variants.

Table 2: Assessments of the signal peptides of CYP2B sub-family and CYP6Z2

CYP	Sequence	P450 Yield (nmol/l)
2B1	MAPSILLLLALLVGFLLLLVRGHPKSRGNFPPGP	20 – 40
2B1Δ3-20	MA KKTSSKGKLPPGP	800 – 1000
2B4	MALLLAVLLAFLAGLLLLLFRGHPKAHGRLPPGP	30 - 40
2B4Δ3-20	MA KKTSSKGKLPPGP	200 – 400
2B6	MALLLAVRLALLTGLLLLLVQRHPNTHDRLPPGP	<1
2B6Δ3-20	MA KKTSSKGKLPPGP	50 – 100
2B11	MALLLAVLLALLTGLLLLMARGHPKAYGHLPPGP	100
2B11Δ3-20	MA KKTSSKGKLPPGP	300 – 600
6Z2	MAVYTLALVAAVIFLVLRYIYSHWERHGLPHLKP	598
6Z2Δ3-13	MA FLVLRYIYSHWERHGLPHLKP	0
6Z2Δ3-25	MA RHGLPHLKP	0

5. Conclusions

This study successfully cloned and expressed the intact 5x His-tagged CYP6Z2 enzyme in *E. coli*, yielding functional P450 holoprotein under specific growth conditions. However, truncated isoforms of CYP6Z2 did not produce functional P450, indicating improper folding and inactivity. Optimal expression was achieved at 30°C with 120 RPM shaking, resulting in the highest P450 yield. The hydrophobic N-terminal region posed challenges in solubilizing the protein, but strategies such as using detergents and modifying the purification protocol improved yield and purity. SDS-PAGE and immunoblotting confirmed the protein's identity and purity. Comparisons with human P450s suggest the importance of the N-terminal signal peptide for proper folding and stability of CYP6Z2. This study highlights the importance of the signal peptide domain in the expression and functionality of insect P450 enzymes.

Authors contributions: Michael Olugbenga Kusimo: Conceptualization, Investigation, Methodology, Project administration. **Taib Ahmed Hama Soor:** Writing – original draft, Writing – review & editing. **Ahmed Adebowale Adedeji:** Designing the idea of the review paper, supervising, reviewing and proof reading, and editing.

Data availability: Data will be available upon reasonable request.

Conflicts of interest: The authors declare that they have no known competing financial interests or personal relationships that could have appeared to influence the work reported in this paper.

Funding: The authors did not receive support from any organization for the submitted work.

References

[1] J. Hemingway and H. Ranson, 'Insecticide resistance in insect vectors of human disease.', *Annu Rev Entomol*, vol. 45, pp. 371–91, 2000, doi: 10.1146/annurev.ento.45.1.371.
[2] WHO, 'World Malaria Report', Geneva, Switzerland, 2023.
[3] WHO, 'Malaria entomology and vector control', Geneva, Switzerland, 2013.
[4] WHO, 'World Malaria Report', Geneva, Switzerland, 2019.
[5] R. T. Jones et al., 'Homology modelling of Drosophila cytochrome P450 enzymes associated with insecticide resistance.', *Pest Manag Sci*, vol. 66, no. 10, pp. 1106–15, Oct. 2010, doi: 10.1002/ps.1986.
[6] I. Karunkeret al., 'Structural model and functional characterization of the Bemisiatabaci CYP6CM1vQ, a cytochrome P450 associated with high levels of imidacloprid resistance.', *Insect Biochem Mol Biol*, vol. 39, no. 10, pp. 697–706, Oct. 2009, doi: 10.1016/j.ibmb.2009.08.006.
[7] P. Lertkiatmongkol, E. Jenwitheesuk, and P. Rongnoparut, 'Homology modeling of mosquito cytochrome P450 enzymes involved in pyrethroid metabolism: insights into differences in substrate selectivity', *BMC Res. Notes.*, vol. 4, pp. 321, Sep. 2011, doi: 10.1186/1756-0500-4-321.
[8] L. A. Mclaughlin et al., 'Characterization of inhibitors and substrates of Anopheles gambiae CYP6Z2', Insect Mol Biol, vol. 17, no. 2, pp. 125–135, Apr. 2008, doi: 10.1111/j.1365-2583.2007.00788.x.

[9] T.-L. Chiu, Z. Wen, S. G. Rupasinghe, and M. A. Schuler, 'Comparative molecular modeling of Anopheles gambiae CYP6Z1, a mosquito P450 capable of metabolizing DDT', *Proceedings of the National Academy of Sciences*, vol. 105, no. 26, pp. 8855–8860, Jul. 2008, doi: 10.1073/pnas.0709249105.

[10] L. M. Podust, T. L. Poulos, and M. R. Waterman, 'Crystal structure of cytochrome P450 14alpha -sterol demethylase (CYP51) from Mycobacterium tuberculosis in complex with azole inhibitors', *Proc. Natl. Acad. Sci. USA,* vol. 98, no. 6, pp. 3068–73, Mar. 2001, doi: 10.1073/pnas.061562898.

[11] E. E. Scott, M. Spatzenegger, and J. R. Halpert, 'A truncation of 2B subfamily cytochromes P450 yields increased expression levels, increased solubility, and decreased aggregation while retaining function.', *Arch. Biochem .Biophys.*, vol. 395, no. 1, pp. 57–68, Nov. 2001, doi: 10.1006/abbi.2001.2574.

[12] U. Heinemann, K. Büssow, U. Mueller, and P. Umbach, 'Facilities and methods for the high-throughput crystal structural analysis of human proteins', *Acc. Chem. Res.*, vol. 36, no. 3, pp. 157–163, Mar. 2003, doi: 10.1021/ar010129t.

[13] R. C. Stevens, 'Design of high-throughput methods of protein production for structural biology', *Structure*, vol. 8, no. 9, pp. R177–R185, Sep. 2000, doi: 10.1016/S0969-2126(00)00193-3.

[14] J. Kaur, A. Kumar, and J. Kaur, 'Strategies for optimization of heterologous protein expression in *E. coli*: Roadblocks and reinforcements', *Int. J. Biol. Macromol.*, vol. 106, pp. 803–822, Jan. 2018, doi: 10.1016/j.ijbiomac.2017.08.080.

[15] Esteves, Francisco, José Rueff, and Michel Kranendonk, 'The central role of cytochrome P450 in xenobiotic metabolism—a brief review on a fascinating enzyme family', *J. Xenobiot.*, vol. 11, no. 3, pp. 94-114, Jun. 2021, doi: 10.3390/jox111030007.

[16] W. Pamela A., Jose Cosme, Vandana Sridhar, Eric F. Johnson, and Duncan E. McRee. 'Mammalian microsomal cytochrome P450 monooxygenase: structural adaptations for membrane binding and functional diversity', *Mol. Cell*, vol. 5, no. 1, pp. 121-131, Jan. 2000, doi: 10.1016/s1097-2765(00)80408-6

[17] T. L. Poulos and E. F. Johnson, 'Structures of Cytochrome P450 Enzymes', in Cytochrome P450, Cham: Springer International Publishing, pp. 3–32, 2015, doi: 10.1007/978-3-319-12108-6_1.

[18] W. Reichhart, Danièle, and René Feyereisen, 'Cytochromes P450: a success story'. *Genome Biol.*, vol. 1, no. 6, pp. 1-9, Dec. 2000, doi: 10.1186/gb-2000-1-6-reviews3003.

[19] J. Cosme and E. F. Johnson, 'Engineering Microsomal Cytochrome P450 2C5 to Be a Soluble, Monomeric Enzyme', *J. Biol. Chem*, vol. 275, no. 4, pp. 2545–2553, Jan. 2000, doi: 10.1074/jbc.275.4.2545.

[20] W. Bo, Li-Ping Yang, Xiao-Zhuang Zhang, Shui-Qing Huang, Mark Bartlam, and Shu-Feng Zhou, 'New insights into the structural characteristics and functional relevance of the human cytochrome P450 2D6 enzyme', *Drug Metab. Rev.*, vol. 41, no. 4, pp. 573-643, Nov. 2009, doi: 10.1080/03602530903118729.

[21] G. A. Schoch, J. K. Yano, M. R. Wester, K. J. Griffin, C. D. Stout, and E. F. Johnson, 'Structure of human microsomal cytochrome P450 2C8. Evidence for a peripheral fatty acid binding site.', *J. Biol. Chem.*, vol. 279, no. 10, pp. 9497–503, Mar. 2004, doi: 10.1074/jbc.M312516200.

[22] M. R. Wester, E. F. Johnson, C. Marques-Soares, P. M. Dansette, D. Mansuy, and C. D. Stout, 'Structure of a substrate complex of mammalian cytochrome P450 2C5 at 2.3 A resolution: evidence for multiple substrate binding modes.', *Biochem.*, vol. 42, no. 21, pp. 6370–9, Jun. 2003, doi: 10.1021/bi0273922.

[23] P. A. Williams, J. Cosme, A. Ward, H. C. Angove, D. Matak Vinković, and H. Jhoti, 'Crystal structure of human cytochrome P450 2C9 with bound warfarin', *Nature*, vol. 424, no. 6947, pp. 464–8, Jul. 2003, doi: 10.1038/nature01862.

[24] J. K. Yano, M. R. Wester, G. A. Schoch, K. J. Griffin, C. D. Stout, and E. F. Johnson, 'The structure of human microsomal cytochrome P450 3A4 determined by X-ray crystallography to 2.05-A resolution.', *J. Biol. Chem.*, vol. 279, no. 37, pp. 38091–4, Sep. 2004, doi: 10.1074/jbc.C400293200.

[25] N. Kruger, 'The Bradford Method for Protein Quantitation' In: Walker, J.M. (eds) The Protein Protocols Handbook. Springer Protocols Handbooks, Humana Press, Totowa, NJ, pp. 17-24, 2009, doi.org/10.1007/978-1-59745-198-7_4.

[26] R. Ceccarelli EA,' Recombinant protein expression in Escherichia coli: advances and challenges', *Front. Microbiol.*, vol 5, pp 172, Apr. 2014, doi: 10.3389/fmicb.2014.00172.

[27] W. Benjamin, and A. Sali, 'Comparative protein structure modeling using MODELLER' *Curr.Bioinform.*, vol 54, no. 1, pp 5-6, Jun. 2016, doi: 10.1002/cpbi.3.

[28] S. Martin, Veronika Navrátilová, Markéta Paloncýová, Václav Bazgier, Karel Berka, Pavel Anzenbacher, and Michal Otyepka, 'Membrane-attached mammalian cytochromes P450: An overview of the membrane's effects on structure, drug binding, and interactions with redox partners', *J. Inorg. Biochem.*, vol 183, pp 117-136, Jun, (2018), doi: 10.1016/j.jinorgbio.2018.03.002.

[29] K. Byron, 'Structural basis for the role in protein folding of conserved proline-rich regions in cytochromes P450', *Toxico Appl Pharmacol.*, vol 199, no. 3, pp 305-315, Sep. 2004, doi: 10.1016/j.taap.2003.11.030.

[30] M. Caroline S., Tobias WB Ost, Michael A. Noble, Andrew W. Munro, and Stephen K. Chapman, 'Protein engineering of cytochromes P-450', *Biochim. Biophys. Acta.*, vol 1543, no. 2 pp 383-407, Dec. 2000, doi: 10.1016/s0167-4838(00)00236-3.

[31] N. T. Southall, K. A. Dill, and A. D. J. Haymet, 'A View of the Hydrophobic Effect', *J. Phys. Chem B.*, vol. 106, no. 3, pp. 521–533, Jan. 2002, doi: 10.1021/jp015514e.

[32] H. Johanna, Heidi Halbwirth, and Oliver Spadiut, 'Recombinant production of eukaryotic cytochrome P450s in microbial cell factories', *Biosci. Rep.*, vol 38, no. 2, Mar. 2018, doi: 10.1042/BSR20171290.

[33] I. H. Hanna, J. R. Reed, F. P. Guengerich, and P. F. Hollenberg, 'Expression of human cytochrome P450 2B6 in Escherichia coli: characterization of catalytic activity and expression levels in human liver.', *Arch. Biochem. Biophys.*, vol. 376, no. 1, pp. 206–16, Apr. 2000, doi: 10.1006/abbi.2000.1708.

[34] P. Michal, Christoph Crocoll, Mohammed Saddik Motawie, and Barbara Ann Halkier, 'Systematic engineering pinpoints a versatile strategy for the expression of functional cytochrome P450 enzymes in Escherichia coli cell factories' *Microb. Cell Fact.*, vol. 22, no. 1, pp 219, Oct. 2023, doi: 10.1186/s12934-023-02219-7.

[35] H. Ramanujan S., and Robert J. Keenan, 'The mechanisms of integral membrane protein biogenesis', *Nat. Rev. Mol. Cell Biol*, vol. 23, no. 2, pp 107-124, Feb. 2022, doi: 10.1038/s41580-021-00413-2.